COINCIDENCE TECHNIQUES IN ATOMIC AND SURFACE ANALYSIS SPECTROSCOPY

JOHN L. ROBINS

Department of Physics, The University of Western Australia, Nedlands, Perth, W.A. 6907 Australia

The information obtainable from electron and X-ray spectroscopy studies can be increased significantly by the use of coincidence techniques. This entails detecting pairs of electrons and/or photons which are scattered or emitted from the same interaction event. This is illustrated by reference to Auger photoelectron coincidence spectroscopy. Some of the techniques currently being developed for enhancing the collection and display of coicidence data in atomic analysis spectroscopy are described. These include the use of microchannel plates and position sensitive detectors to provide parallel data collection of coincidence measurements. These can offer at least two orders of magnitude reduction in data collection time and lead to both energy dispersive and momentum dispersive displays in (e,2e) analyses. The possibility of using these procedures for surface and thin film analysis is discussed.

1. Introduction

Many analysis techniques used in atomic, surface and solid state studies involve bombarding a targe with a well characterised beam of electrons, atoms, ions, or photons and then analysing the particles or photons which are emitted. From this analysis, conclusions are drawn about the interaction process and, hence, the prop-

erties of the target material. The detection of the emitted particles can be carried out with a single analyser and this is probably the most common procedure.

However, if the interaction produces two or more particles, then additional information can be gained from the analysis, depending on how many of these particles can be detected and characterised. Mounting two analysers is usually not a major problem. More difficult is the task of determining, of all the particles entering the two detectors, which pairs have originated from the same event. This can be done by precise timing, as such a pair will be detected within a few nanoseconds of each other, allowing for slightly different transit times to and through the detectors. This is referred to as coincidence detection and could apply to two or more particles.

Recently, considerable progress has been made in developing enhanced data collection and analysis techniques in the field of (e,2e) spectroscopy which inherently involves coincidence detection of pairs of electrons. These developments will be described here and it is hoped that they may find increased application in the field of surface analysis in the future. The description of these techniques will be given in Section 4 after the basic concepts of coincidence spectroscopy have been reviewed in Section 2 and illustrated with reference to Auger spectroscopy in Section 3.

2. Coincidence techniques

Many analytical techniques which involve scattering result in the emission of two or more particles or photons. Coincidence spectroscopy involves detecting two or more of these which have been emitted within a sufficiently short time interval that the two particles can be expected to have arisen from the same event. Of course, some such 'coincidence' detections may result from entirely separate events which happen to emit particles with appropriate energies into the collection area of the two detectors within the prescribed time interval. Elimination of these random coincidences has to be achieved by statistical analysis.

These statistical requirements, plus the low probability that an event will result in both the emitted particles entering the collection areas of the detectors, lead to the necessity for either very high intensity excitation sources or extremely long data collection times (often weeks for a given spectrum). The latter puts special requirements on the equipment including long term stability. In both cases there is also a need for high resolution timing to minimise the number of random events recorded.

The basic electronics required for coincidence rate measurements is described in a paper by Thurgate [1]. In essence, the nanosecond pulse signals from two detectors are fed to a time-to-amplitude converter (TAC) to measure the time between one particle arriving in the start-channel and another arriving in the stop-channel. In practice, the signal to the stop–channel is delayed so that random events, arriving with time separations either side of the true coincidences, show the background due to random coincidences. It can be assumed that this background in the TAC spectrum extends through the time interval in which true coincidences occur and, hence, by subtraction, the true coincidence peak can be determined. For each

pair of energies, counting is continued until the true coincidences recorded show a statistically significant peak above the background of random coincidences. This requirement also contributes to the long run times.

3. An illustration of coincidence spectroscopy

The value of coincidence techniques can be illustrated by reference to Auger analysis as will be shown in this section, the contents of which formed part of a recent review by the author on Auger photoelectron coincidence spectroscopy [2].

In the Auger process, an atom is ionised by removal of an inner shell electron through either electron or photon bombardment. This is followed by an electron from a higher level 'falling' into the inner shell vacancy. This leaves the atom still ionised but in a lower energy state. The excess energy is removed either by the emission of a photon (fluorescence) or by the emission of an electron from one of the higher energy levels (Auger process). It is thus clear that in the photon stimullated Auger process, two electrons, one being the ejected photoelectron and the other being the Auger electron itself, are emitted simultaneously and the process lends itself to the use of coincidence techniques.

It is common to use the word singles to distinguish the normal Auger spectrum from a coincidence spectrum. For the normal spectrum there is only one detector and, for example, the energy distribution of all emitted Auger electrons is recorded. In a coincidence spectrum, with two or more detectors, two or more electrons are detected in coincidence. A typical coincidence spectrum might be the energy distribution of only those Auger electrons detected in coincidence with photoelectrons of a specified energy.
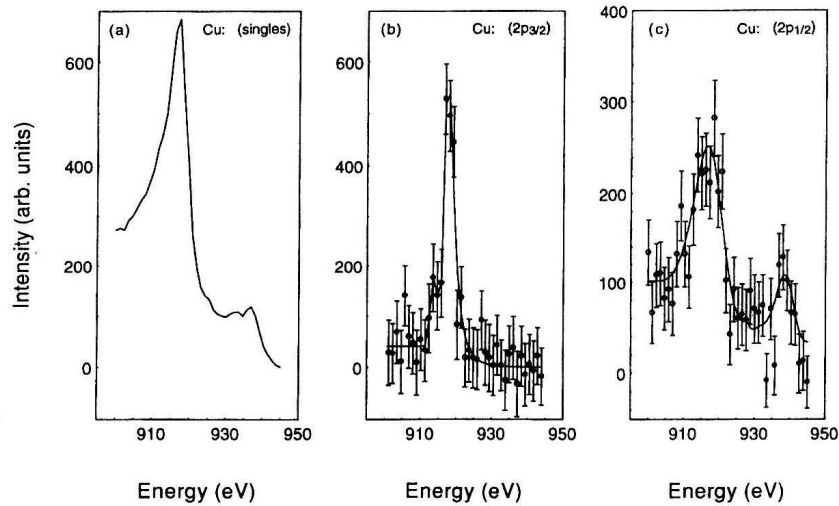

Fig. 1. Copper $L_{23}VV$ Auger spectra; (a) singles, and in coincidence with the (b) $2p_{3/2}$ and (c) $2p_{1/2}$ photoelectrons [1].

Figure 1a shows a copper $L_{2,3}$VV singles spectrum recorded by Thurgate et al. [1, 3]. Two main peaks at about 939 eV and 918 eV are interpreted as the L_2VV and L_3VV Auger peaks, respectively. It is clear that these peaks are broadened, especially on the low energy side, and there are satellite peaks in the spectrum. In fact, as will be described later, coincidence spectroscopy will show that part of the broad L_3VV peak at 918 eV is due to an initial L_2 shell ionisation followed by a Coster-Kronig transition before the Auger process proceeds. Similarly, part of the peak at about 934 eV has its origin in L_1 level ionisation, followed by a Coster-Kronig transition prior to the Auger emission.
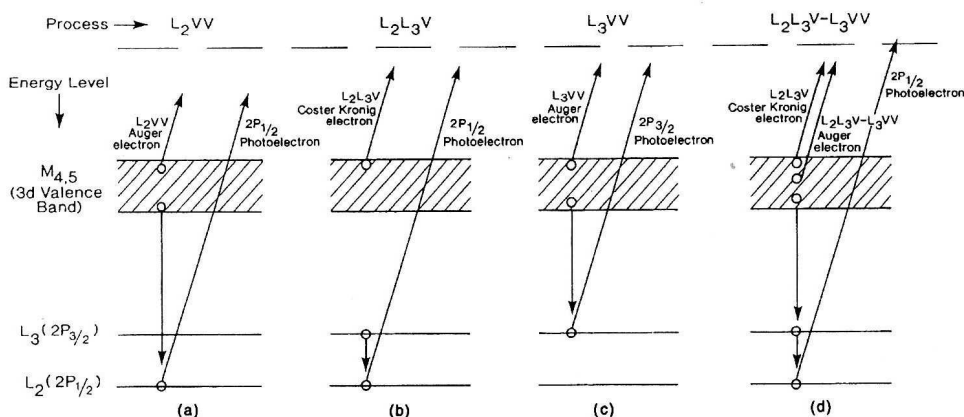

Fig. 2. Processes responsible for some peaks in the L_{23}VV Auger spectra of copper [4].

The basic Auger emission events which lead to the emission of an L_2VV Auger electron in copper are illustrated in Fig. 2a [4]. The emitted electrons are the $2p_{1/2}$ (or L_2) photoelectron and L_2VV Auger electron. The latter will have an energy of about 938 eV and is responsible for the peak at this energy in the copper spectrum shown in Fig. 1a. The events leading to the emission of an L_3VV Auger electron are shown in Fig. 2c and these Auger electrons contribute to the peak at 918 eV in Fig. 1a. These energies reflect the fact that the photoelectron leaves an atom with a vacancy in the L_2 (or L_3) level, that the valence electron makes its transition between energy levels in a singly ionised atom, and the Auger electron is emitted from an atom with a hole in the valence band. The final energy of the Auger electron is governed by the binding energies which are appropriate to the state of the atom as the transition occurs.

A Coster-Kronig transition involves the rapid transition of an electron between two adjacent levels within the same shell in an atom with the excess energy being removed through emission of another electron, usually from a higher energy state. In terms of the events illustrated in Fig. 2a, we may imagine a Coster-Kronig transition occurring immediately after the formation of the hole in the L_2 level (as

shown in Fig. 2b), but before the Auger electron is emitted. The total process is shown schematically in Fig. 2d.

It is helpful to think of this as a three–step process in order to clarify the following points. The initial ionisation, which creates a hole in the L_2 level, is a standard ionisation process. The Coster-Kronig process then involves the transition of an L_3 electron into the L_2 vacancy with the excess energy being removed by emission of a valence electron, leaving a vacancy in the valence band. The Auger process then proceeds as if it were an L_3VV process, as it is using a vacancy which now exists in the L_3 level. Such a combined process will be referred to as an L_2L_3V-L_3VV process. However, the emitted Auger electrons will not have exactly the same energy as the L_3VV Auger in Fig. 2c, as the energy levels involved will be modified by the presence of the additional vacancy in the valence band. These Auger electrons thus contribute to a peak which occurs close in energy to the L_3VV peak but is associated with L_2 (not L_3) ionisation and, hence, will occur in coincidence with $2p_{1/2}$ (and not $2p_{3/2}$) photoelectrons. This is confirmed by coincidence Auger spectroscopy.

The coincidence Auger spectra of copper [1,3] are shown in Fig. 1b and 1c. Figure 1b is the spectrum in coincidence with $2p_{3/2}$ photoelectrons and so shows only those processes which are associated with initial ionisation of the L_3 level. Figure 1c is the spectrum in coincidence with $2p_{1/2}$ photoelectrons and, hence, shows processes associated with initial ionisation in the L_2 level. Clearly, the peak at about 919 eV in Fig. 1c cannot be the basic L_3VV Auger peak which arises from initial L_3 level ionisation. Rather, it arises from initial L_2 level ionisation, followed first by a Coster-Kronig L_2L_3V process and then by an Auger process using the L_3 vacancy. Namely, it is the L_2L_3V-L_3VV process. This results in a peak which is close to, but slightly shifted (by about 2.5 eV) from, the regular L_3VV peak seen in Fig. 1b.

It is also seen that the peak at about 934 eV in the singles spectrum of Fig. 1a does not appear in the coincidence $L_2VV(2p_1/2)$ spectrum of Fig. 1c. This is because the 934 eV peak originates from ionisation in the L_1 level. It is due to a Coster-Kronig related transition, namely L_1L_2V-L_2VV. There may also be some contribution to the spectrum at this energy from a final state shake-up/off [5].

This illustrates just one of the values of coincidence spectroscopy. In this case it has clarified the origin of the peaks which appear related because of juxtaposition in the singles spectrum but which have significantly different origins.

4. New data analysis techniques

Recently, new powerful detection and data handling techniques have been developed which can reduce data collection times and should be applicable to many coincidence experiments [6-8]. As these are currently being developed for use with the analysis technique referred to as (e,2e), a brief description of this technique is presented here.

The (e,2e) technique is applicable to the study of electron-electron scattering

[9]. Electrons of well defined energy E_0 and momentum $\vec{p}_0$ impinge upon target atoms and ionising collisions take place with electrons within these atoms. The energies (E_1 and E_2) and the momenta ($\vec{p}_1$ and $\vec{p}_2$) of the two emitted electrons (one scattered and the other ejected) are measured. This permits calculation of the binding energy $E_b = (E_0 - E_1 - E_2)$ and the recoil momentum $\vec{p} = (\vec{p}_0 - \vec{p}_1 - \vec{p}_2)$.

In simple geometries, with high incident energies, where plane wave approximations are valid, the recoil momentum $\vec{p}$ is equal and opposite to the momentum $\vec{q}$ of the target electron at the instant of collision. By measuring the momenta $\vec{p}_1$ and $\vec{p}_2$ over a range of emitted directions, all components of the momentum $\vec{q}$ of the target electron can be determined and hence the energy-momentum density of the electron within the atom can be determined. For this reason such experimets are allternatively referred to as electron momentum spectroscopy (EMS).

This technique is more easily applied to gas targets and so has its widest application in atomic and molecular physical chemistry. However, there is increasing activity in trying to apply the technique to surface analysis and this will be discussed later. The new detection and data handling techniques being used in EMS are described below.

4.1. Enhanced energy analysis

The enhanced energy analysis uses the fact that when a beam of electrons with an energy spread enters a hemispherical energy analyser, the radii of the paths traversed by electrons are a function of their energy [6]. Thus the beam is dispersed radially as it exits the analyser. Conventionally, electrons of a chosen energy are sequentially deflected onto a single exit slit aperture and counted by a single detector, such as a channeltron, mounted behind it.

One might imagine a number of exit apertures, arranged radially, each with a separate counter, being used concurrently to collect data for a number of energies. This priciple can be carried further [6] by replacing all of the exit apertures with a narrow radial slit behind which is mounted a position sensitive detector (PSD). This may consist of a stack of two or three microchannel plates (MCPs) backed by a resistive anode position detector. Hence, the dispersed energy spectrum can be recorded simultaneously along the radial exit slit. In addition, both a timing and a strobe pulse can be generated from the channel plate each time an electron is detected and the energy of this electron is given by the position coordinate on the detector.

In coincidence spectroscopy, two such detectors are employed and coincidence events are recognised and recorded [7] by a procedure which is an extension of that described in Section 3. The timing pulse from one detector starts a time-to-analogue converter (TAC) whilst the pulse from the other stops it. (See Fig. 3). If these events occur within an interval of about 50 ns, the conversion is initiated and another strobe pulse in generated. The time delay introduced into the output also allows synchronisation of the time and position data. If there is a triple coincidence of the three strobe pulses, the two energies and the time difference are forwarded to the histogramming board where they are digitised to a single data element which

is used as an address in the computer's memory. Histogramming is achieved by increasing the number stored in that address by one each time that address is generated.
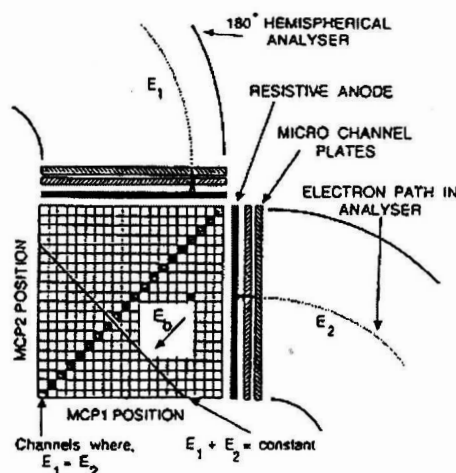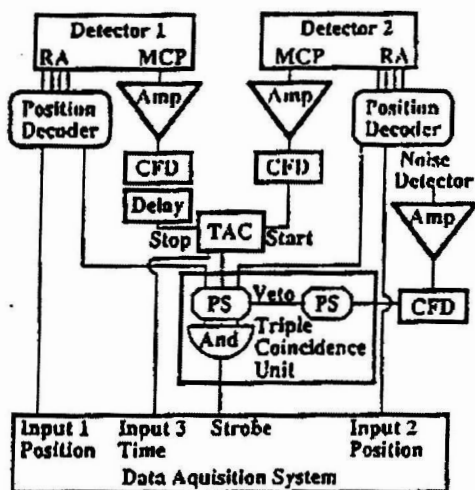

Fig. 3. Schematic diagram of the coincidence timing electronics [7].

Fig. 4. Two-dimensional energy grid formed by the microchannel plates of two analysers (MCP1,2). Each microchannel plate produces an energy coordinate for a coincidence event, and the shaded channels indicate equal electron energies. Lines of equal binding energy (E_b) run perpendicular to this diagonal [6] (right).

A histogram is shown schematically in Fig. 4 and typically consists of a 32 x 32 energy grid with the axes being defined by the exit slits of the detectors [6]. Within each grid cell, the TAC data for the given pair of energies E_1 and E_2 are stored. This number versus time interval TAC spectrum allows separation of the random and true coincidence events. In effect, data for over 1000 (i.e. 32 x 32) pairs of energy settings of two conventional energy analysers are collected simultaneously. For a symmetric (e,2e) experiment (directions of emitted electrons symmetric about the direction of the incident beam), the binding energy ($E_b = E_0 - E_1 - E_2$) will be constant for constant values of ($E_1 + E_2$). This corresponds to a straight line across the E_1, E_2 grid surface, as shown in Fig. 4. Using data from argon, the true coincidence rates are plotted on the three–dimensional representation shown in Fig. 5. The regions where ($E_1 + E_2$), and hence E_b, are constant are along diagonals from top right to bottom left, and these can be clearly distinguished. By summing and averaging along these diagonals, the binding energy spectrum for argon, as shown in Fig. 6, can be generated. Further details of additional information which can be gained from this coincidence data can be founds in the literature [6,7].
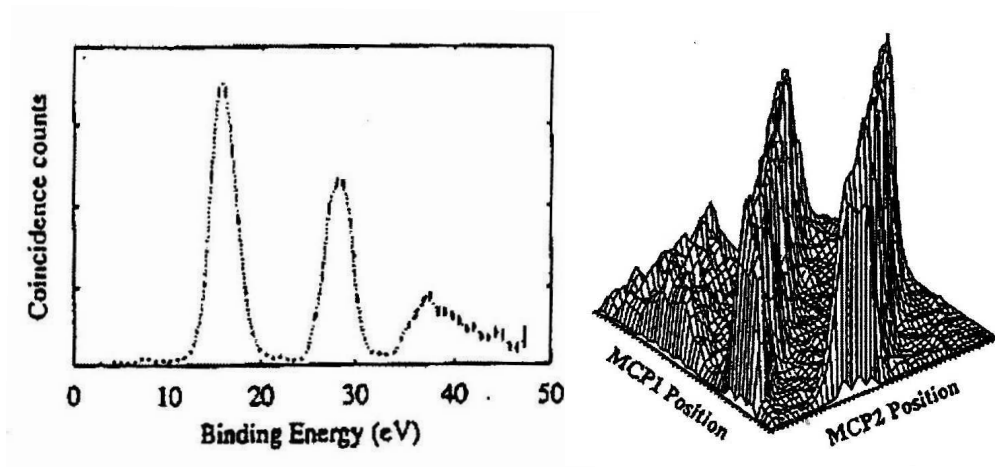
Fig. 5. Three-dimensional histogram of coincidence counts on the energy grid shown in Fig. 4 [7].

Fig. 6. Binding energy spectrum of argon derived from Fig. 5 [7] (right).

In this application of microchannel plate position sensitive detectors, only one dimensional strips of the plates are used as only the linearly dispersed energy distribution is analysed. In the next subsection it will be shown how such plates can be used for energy and direction dispersion measurements.

4.2. Enhanced energy and direction analysis

Using a toroidal electrostatic energy analyser [10], electrons scattered coplanar with the entrance slit can be focused in the output plane. Electrons of the same energy, which have been scattered through most angles between 0° and 360 °, can be selected and focused onto a circular line image. Also, as energy dispersion is radial, with appropriate output optics and a two–dimensional position sensitive detector it is possible to image both the direction and energy dispersions (i.e. the momentum dispersion) of the selected electrons [11].

For use with (e,2e) experiments on the impact ionisation of atoms, a group at the University of Western Australia has built a pair of coaxial toroidal electrostatic electron energy analysers [8]. This permits coincidence detection of pairs of electrons which have been generated in a nonsymmetric mode in which one is a fast, principally forward scattered, electron and the other is a slower ejected electron. A cut-away section of the analyser is shown in Fig. 7. Electrons moving in the negative x-direction impinge on gas target atoms at the coordinate origin and in principle all electrons ejected into the 360° of the $x--y$ plane (normal to the plane

of the figure) will be focused onto the plane of the MCP position sensitive detector. This detector consists of a stack of two microchannel plates backed by a resistive anode, as discussed above. The more energetic scattered electrons are focused by the outer toroidal analyser and, as these are principally scattered in the forward direction, a limited number of single detectors, located at discrete angles, are used for their detection.
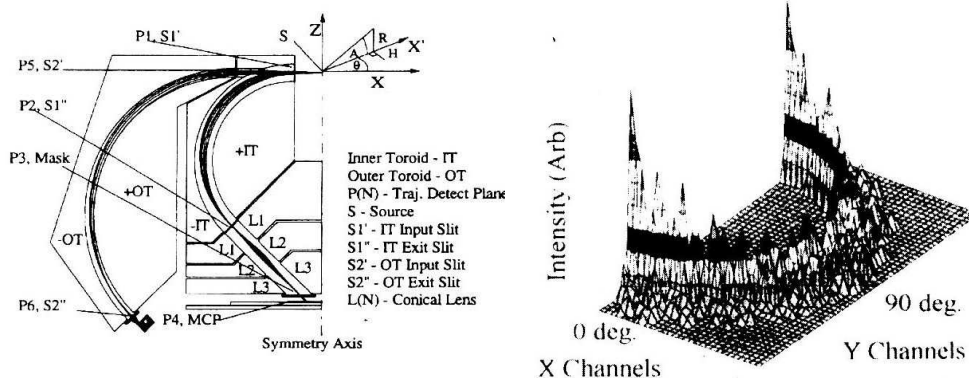

Fig. 7. Schematic diagram of inner and outer toroids, trajectories and coordinates of the pair of coaxial toroidal electron energy analysers [8].

Fig. 8. Modelled image of intensity versus energy and direction for electrons ejected during impact ionisation of an extended gas source, and collected in the inner toridal analyser of Fig. 7 [8] (right).

Extensive modelling of this analyser has been carried out [8] to permit optimisation of the rather complex array of parameters. Figure 8 shows the modelled image of intensity versus energy and direction for electrons ejected during impact ionisation of a gas such as argon. Such images need further correction to allow for the extended, rather than point, nature of the scattering source. These analysers were used to obtain the data shown in Fig. 9, which represent the distribution of 103 eV electrons emitted during impact ionisation of argon by 1118.7 eV electrons directed along the 0° axis. The emitted electrons were detected in coincidence with 1000 eV electrons scattered through 4°. The double peaked forward emission is indicative of p state electrons and the backward emission is believed to arise from ion repulsion [12].
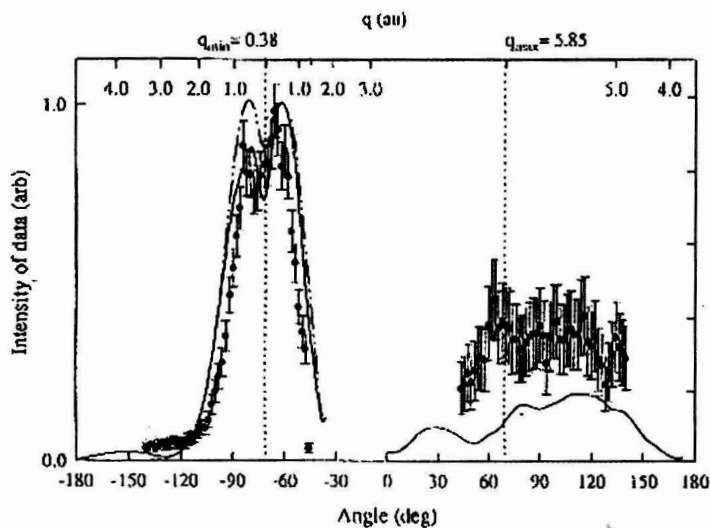
Fig. 9. Angular distribution of 103 eV electrons emitted in coincidence with the electrons scattered through 4° with energy 1000 eV, during impact ionisation of argon by 1118.7 eV electrons. The data points are compared with calculated cross sections using the plane-wave impulse approximation (broken line) and the distorted wave impulse approximation (full line) [12].

5. Application to surface analysis

As coincidence measurements, such as the (e,2e) studies discussed above, involve the relative directions of the incident and emitted electrons, it is essential that no unknown scattering of these electrons takes place either before impact or before detection. This creates considerable problems when applying the (e,2e) analysis technique to the study of solids. Some success has been achieved with very thin solid targets, either self supporting or layers on a thin substrate, using the transmission configuration [9,13-15]. Relatively high energy (say 20 keV) electrons have sufficiently long mean free paths in light elements, such as aluminium or carbon, to traverse films of about 10 nm thickness. If the geometry is such that the scattered and ejected electrons chosen for detection have energies of about 18.8 keV and 1.2 keV, respectively, then any coincidence events detected will have occurred within about 1–2 nm of the exit surface, due to the short mean free path of the 1.2 keV electrons. Such studies have been carried out on a range of low atomic number solids using the techniques described above to reduce the data collection times [9,16].

It would appear that true surface analysis will require the use of the reflection geometry, although the cross-section for backscattering during electron impact ionisation is usually very low. The theory for reflection coincidence experiments using grazing incidence was presented back in 1978 [17]. However, it would appear that

the first relatively successful application of this technique has only recently been reported. This was the work of Iacobucci et al. [18] which involves a grazing incidence beam of very low energy (300 eV) electrons to ensure surface analysis. The surface studied was clean highly oriented pyrolitic graphite. A hemispherical energy analyser was used to detect the forward scattered electrons which just emerge from the surface, and a cylindrical mirror energy analyser aligned normal to the surface was used to detect the ejected electrons. At present none of the enhanced detection techniques discussed here have been employed. However, the achievement of binding energy analysis with moderate quasi momentum discrimination is an encouraging indication that electron momentum spectroscopy of electrons in surface atoms in solids may be possible in the near future.

6. Conclusion

The use of coincidence techniques can greatly enhance the information gained from some surface analytic spectroscopies, as illustrated by Auger photoelectron coincidence spectroscopy. However, a major problem with such techniques is the inherent low count rate and corresponding long data collection times with conventional detection methods.

It has been shown that the use of positon sensitive detectors allows simultaneous collection of data from a range of scattering events. The use of these techniques in coincidence spectoscopy can reduce data collection times by one to two orders of magnitude. These detectors also allow energy distributions and even momentum distributions to be obtained directly in certain circumstances. Whilst these newer techniques have been initially developed for atomic spectroscopies, their eventual use in surface spectroscopies should be possible.

Acknowledgements

References

1) S. Thurgate, B. Todd, B. Lohmann and A. Stelbovics, Rev. Sci. Instrum. **61** (1990) 3733;

2) J. L. Robins, Prog. Surf. Sci. **48** (1995), 167;

3) S. M. Thurgate, Aust. J. Phys. **43** (1990) 443;

4) S. M. Thurgate, in *The Structure of Surfaces III*, eds. S.Y. Tong, M.A. Van Hove, K. Takayami and X.D. Xie, (Springer-Verlag, Berlin, 1991) p 179;

5) S. M. Thurgate and J. Neale, Surf. Sci. Lett. **256** (1991) L605;

6) P. Hayes, M. A. Bennett, J. Flexman and J. F. Williams, Rev. Sci. Instrum. **59** (1988) 2445;

7) M. A. Bennett, P. A. Smith, D. K. Waterhouse, M. J. Ford, J. Flexman and J. F. Williams, Rev. Sci. Instrum. **63** (1992) 1922;

8) J. H. Flexman, J. F. Williams and P. A. Hayes, Journ. de Physique IV: Suppl. J. de Physique II **3** (1993) 79;

9) I. E. McCarthy and E. Weigold, Contemp. Phys. **35** (1994) 377;

10) R. Leckey, J. Electron Spectrosc. Rel. Phenom. **43** (1987) 183;

11) R. Leckey, J. D. Riley and A. Stampl, J. Electron Spectrosc. Rel. Phenom. **52** (1990) 855;

12) J. H. Flexman and J. F. Williams, private communication;

13) M. Vos, P. Storer, Y. Q. Cai, A. Kheifets, I. E. McCarthy and E. Weigold, J. Phys. C; Condensed Matter **7** (1995) 279;

14) M. Vos, P. Storer, S. A. Canney, A. S. Kheifets, I. E. McCarthy and E. Weigold, Phys. Rev. B **50** (1994) 5635;

15) Y. Q. Cai, M. Vos, P. Storer, A. S. Kheifets, E. I. McCarthy and E. Weigold, Phys. Rev. B **51** (1995) 3449;

16) J. F. Willliams and P. A. Hayes, Aust. J. Phys. **43** (1990) 465;

17) A. D'Andrea and R. Del Sole, Surf. Sci. **71** (1978) 306;

18) S. Iacobucci, L. Marassi, R. Camilloni, S. Nannarone and G. Stefani, Phys. Rev. Lett., (to be published).

SUDESNA MJERENJA U ATOMSKOJ SPEKTROSKOPIJI I ANALIZAMA POVRŠINA

Primjena sudesne metode u elektronskoj i rendgenskoj spektroskopiji omogućuje dobivanje znatno vrednijih eksperimentalnih podataka. Promatraju se parovi elektrona i/ili fotona koji su emitirani ili raspršeni u jednom događaju. Ova se metoda ilustrira Augerovom sudesnom spektroskopijom. Opisuju se neke nove metode za poboljšavanje sakupljanja podataka, kao mikrokanalne pločice i položajno osjetljivi detektori. Njima se brzina sabiranja podataka povećava i za više od dva reda veličine i omogućuje istovremena energijska i impulsna disperzijska analiza (e,2e) procesa. Raspravljaju se mogućnosti primjene tih metoda u istraživanju površina i tankih slojeva.